PNAS RESEARCH ARTICLE | POPULATION BIOLOGY OPEN ACCESS

Disentangling the causes of mumps reemergence in the United States

Deven V. Gokhale[a,b,c,1], Tobias S. Brett[a,b,c], Biao He[d], Aaron A. King[e,f], and Pejman Rohani[a,b,c]

Edited by Alan Hastings, University of California Davis, Davis, CA; received May 2, 2022; accepted November 19, 2022

Over the past two decades, multiple countries with high vaccine coverage have experienced resurgent outbreaks of mumps. Worryingly, in these countries, a high proportion of cases have been among those who have completed the recommended vaccination schedule, raising alarm about the effectiveness of existing vaccines. Two putative mechanisms of vaccine failure have been proposed as driving observed trends: 1) gradual waning of vaccine-derived immunity (necessitating additional booster doses) and 2) the introduction of novel viral genotypes capable of evading vaccinal immunity. Focusing on the United States, we conduct statistical likelihood-based hypothesis testing using a mechanistic transmission model on age-structured epidemiological, demographic, and vaccine uptake time series data. We find that the data are most consistent with the waning hypothesis and estimate that 32.8% (32%, 33.5%) of individuals lose vaccine-derived immunity by age 18 y. Furthermore, we show using our transmission model how waning vaccine immunity reproduces qualitative and quantitatively consistent features of epidemiological data, namely 1) the shift in mumps incidence toward older individuals, 2) the recent recurrence of mumps outbreaks, and 3) the high proportion of mumps cases among previously vaccinated individuals.

mumps | vaccine failure | epidemiological model | statistical inference

Significance

Mumps is a vaccine-preventable childhood infection that has undergone a resurgence in many developed countries boasting high immunization coverage. The recent reemergence of this viral infection, once considered a candidate for eradication, has raised suspicions regarding the effectiveness of current vaccines. There are also outstanding questions about why the mumps vaccine has failed to generate population-level immunity. The mechanism underlying vaccine failure has substantive impacts on the development of new vaccines. Here, we confronted multiple epidemiological models of vaccine failure with data from the past three decades in the United States to identify the causative mechanism for mumps emergence. We found waning of vaccine-derived immunity to be the most likely reason for mumps reemergence in the early 21st century US.

The sustained reemergence of mumps in multiple high-vaccine coverage countries, including the United States (1), Canada (2), England (3, 4), South Korea (5), and Denmark (6), over the last two decades is puzzling from a population biological perspective and has raised concerns about the adequacy of current vaccines (7). Mumps is an infectious disease caused by an RNA virus of the family *Paramyxoviridae* (8). While infection in school-aged children is typically mild, with symptoms including inflammation in the salivary glands and fever (8), in postpubescent individuals, infection can cause severe disease, including encephalitis (9), deafness (10), and infertility (11, 12). Prior to routine infant immunization, infection with mumps was viewed as a childhood rite of passage (13), with serological studies from the prevaccination era suggesting that by 14 to 15 y of age, 90% of the population were typically seropositive to mumps antibodies (14, 15). In countries like the United States, routine immunization has been highly successful at substantially reducing mumps incidence by over 99.9% compared to the prevaccine era incidence (7), and it was once considered a candidate for global elimination (15). However, the recent resurgence of mumps in some highly vaccinated populations has cast doubt on the feasibility of this goal (16).

The exact nature of vaccine failure underlying this recent reemergence remains contested (17–19). The two leading hypotheses are that 1) vaccinal immunity against mumps transmission wanes over time (18, 19) and 2) genetic mismatch between vaccine strains and presently circulating viruses has reduced vaccine efficacy (17, 20). There is empirical evidence in support of both hypotheses (21, 22), and given the contrasting policy implications associated with each mechanism, it remains important to pin down the underlying cause of mumps resurgence. With waning vaccine effectiveness, periodic booster immunizations are necessary (18, 23). For a mismatched vaccine, on the other hand, boosters with the same vaccine are typically ineffective and updated vaccines are required (24–27).

In support of the waning hypothesis, longitudinal serological studies have shown that vaccine-derived antibodies decay over time (28); however, there is uncertainty about how this maps onto waning of protective immunity at the population level since serological correlates of protection have not been identified (18). Epidemiological factors consistent with waning immunity include a shift in the age distribution of reported cases to the older age groups (typically 18 to 25 y) (1). Waning of vaccine efficacy can diminish the population-level immune protection thereby increasing the chances of pathogen reestablishment (29–31).

Author contributions: D.V.G., T.S.B., B.H., A.A.K., and P.R. designed research; D.V.G. performed research; D.V.G. analyzed data; and D.V.G., T.S.B., and P.R. wrote the paper.

The authors declare no competing interest.

This article is a PNAS Direct Submission.

[1]To whom correspondence may be addressed. Email: vgdeven@gmail.com.

This article contains supporting information online at http://www.pnas.org/lookup/suppl/doi:10.1073/pnas.2207595120/-/DCSupplemental.

Published January 9, 2023.

In addition, vaccination might be providing incomplete protection referred to as "leaky" protection (30) against present circulating strains. Mumps viruses exhibit substantial phylogenetic diversity, with 13 known genotypic variants identified globally (32). Historical vaccines (such as the original Jeryl Lynn vaccine developed in the United States) are typically derived from prior circulating genotype A viruses. However, the recent resurgent epidemics in the United Kingdom, Canada, and the United States have all been caused by genotype G viruses, indicative of genotype replacement (19). Furthermore, immunological assays suggest reduced cross-neutralization ability of vaccine-derived (genotype A) antibodies against genotype G viruses compared with genotype A (17).

Using the reemergence of mumps in the United States as a case study, in this paper, we aim to determine the putative mechanism of vaccine failure underlying national-level mumps reemergence by performing likelihood-based statistical inference using dynamical transmission models. Transmission models have proven useful in drawing ecological inferences about reemergence of numerous vaccine-preventable childhood infections including measles (33, 34), pertussis (35), influenza (36), and diphtheria (37). Here, we construct an age-structured *SEIR* mechanistic model informed by demographic and vaccine uptake data to test the competing hypotheses regarding vaccine failure. We conduct formal hypothesis testing using age-structured time series of national-level US mumps incidence between the years of 1977 and 2018 sourced from the Centers for Disease Control and Prevention (38, 39). We find that the model with waning vaccine immunity best explains the dynamics in the observed data. Our model is effectively able to reproduce crucial characteristics such as the timing of recent epidemics and the gradual increasing trend in the age distribution of cases to the older age groups.

Results

After the roll-out of infant vaccination (*SI Appendix*, Fig. S3*C*), the United States experienced a pronounced decline in mumps incidence, down to a nadir of 10% of prevaccination levels in 1984 (Fig. 1*A*). However, this decline was interrupted in the mid-1980s, when the United States experienced resurgent outbreaks, with cases concentrated in the 5 to 15 age group (Fig. 1*B* and *C*) (1) with a geographic concentration centered around the mid-western states (Fig. 1*D*) (40). In response, a nationwide vaccine booster campaign was initiated in 1989 (*SI Appendix*, Fig. S3*D* for estimated vaccine uptake data), targeting 4-y-old individuals (13). Subsequently, mumps incidence further declined until a second large outbreak in 2006, which has been followed by sustained transmission ever since (Fig. 1*A*). The majority of post-2006 cases have been aged over 15 y (Fig. 1*C*), and the midwest has again been a geographic focus (Fig. 1*E*). Of potential concern is the observation that most cases have occurred in individuals who have completed the recommended two-dose vaccine schedule (41), leading to speculation about vaccine effectiveness.

Formal Hypothesis Testing. As outlined above, two distinct mechanisms of vaccine failure have been proposed to explain the resurgence of mumps in highly vaccinated countries: 1) transient vaccinal protection (the "waning" hypothesis) and 2) imperfect immunity against genotype G (the "leaky" hypothesis). To formally arbitrate among these putative drivers of mumps reemergence, we formulated an age-structured, two-genotype transmission model that captures each mechanism of vaccine failure (*Materials and Methods*, *SI Appendix*, Eqs. S13–S22).

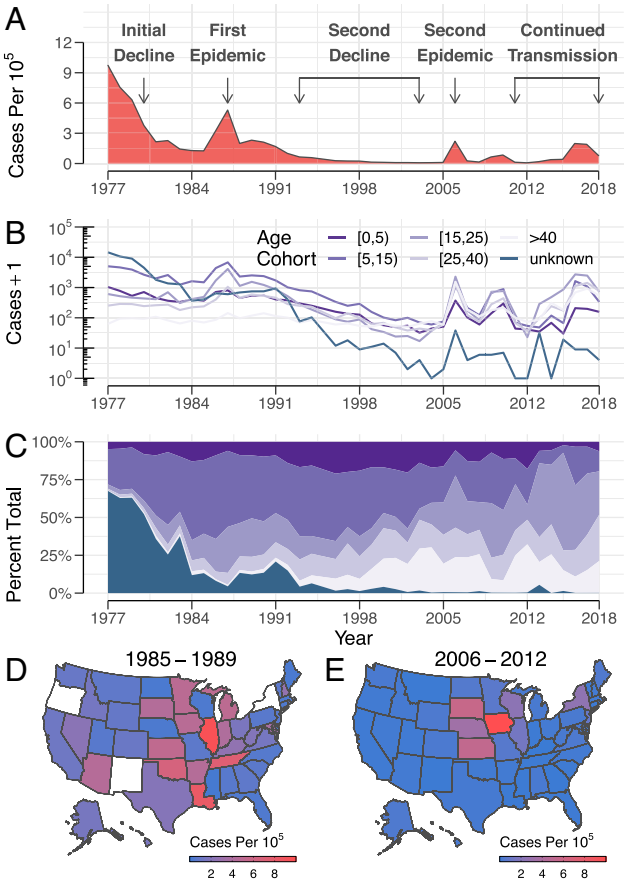

Fig. 1. Mumps distribution in the United States. (*A*) Total reported mumps cases per 10^5. (*B*) Age-stratified case reports across 5 age cohorts (purple gradient). (*C*) Age distribution of mumps case reports (purple gradient); (*D* and *E*) Spatial distribution of average mumps case reports per 10^5 during the two reemergence eras, 1985 to 1989 (panel *D*) and 2006 to 2012 (panel *E*).

We further investigated three models of immune waning. In the first, the duration of vaccinal immunity was assumed to be exponentially distributed (i.e., with no characteristic age at which immunity is lost). In the second and third, motivated by the observation that recent cases were primarily 15 to 25 y old, we modeled the duration of vaccinal immunity using an Erlang distribution, which permits a modal age at which immunity is lost. All hypotheses were compared to a "no-loss" model which assumed perfect, permanent vaccine-derived immunity. Where possible, parameter estimates were obtained from the literature, with unknown epidemiological and immunological parameters were estimated via trajectory matching executed using likelihood-based statistical inference (*Materials and Methods*, for details). Finally, due to missing vaccine uptake data in the period covering the roll-out of booster doses (1989 to 2000), for each model, we compared four qualitatively distinct shapes of booster uptake (constant, sigmoid, convex, and concave; *SI Appendix* for full details).

Among the competing models, we found the exponential waning model provided the best explanation for the observed data, as quantified using the Akaike information criterion (AIC) (Table 1). For this model, we estimated a basic reproductive number, R_0 of 14 (95% CI: 12.6, 15.5), consistent with previous estimates (42). On average, vaccine-derived protection lasts for 111 y (95% CI: 93 y, 144 y). Of the booster uptake shapes, the sigmoidal trajectory provided the best fit to the data (lowest AIC). To compare the performance of vaccination across models,

Table 1. Table of parameter maximum likelihood estimates and derived quantities

	Model				
Parameter/quantity	No loss	Waning (exponential)	Waning (Erlang, N = 2)	Waning (Erlang, N = 3)	Leaky
ΔAIC	207.3	0	17.8	26.9	10.9
$\Delta\log(\mathcal{L}(\Theta))$	22.3	127.0	118.1	113.6	122.6
R_0	42.4	14.0	19.1	31.4	22.2
R_p	0.5	5.7	11.8	18.7	0.8
ξ	0.99	0.59	0.38	0.4	0.97
β_1	0.18	0.04	0.64	0.34	0.74
σ^{-1} (d)	12.0	25.0	25.0	16.9	25.0
δ^{-1} (y)	–	111.5	54.5	56.5	–
ε	–	–	–	–	0.03
t_{intro}	–	–	–	–	2000
Booster shape	Constant	Sigmoid	Sigmoid	Sigmoid	Constant

The symbols in the first column represent the basic reproductive number (R_0), the effective reproductive number calculated at the mean vaccine coverage p (R_p), the population-level vaccine impact ξ, the amplitude of seasonality (β_1), the mean duration of latency (σ^{-1}), vaccine-derived immune duration (δ^{-1}), vaccine leakiness (ε), and the year of genotype G introduction (t_{intro}). Confidence intervals for MLEs are presented in *SI Appendix*, Table S4 and section B.

given the different mechanisms of failure, we followed McLean and Blower (30) and Magpantay et al. (35, 43) and derived a quantification of the vaccine impact (ξ), defined as the reduction in population-level virus transmissibility in the presence of the vaccine. For the exponential waning model and vaccination coverage fixed at the average for 2008 to 2018 (91.7% and 91.6% for the neonatal and the booster, respectively), ξ was estimated to be 59% (95% CI: 54%, 67%).

The remaining model and booster shape combinations were ranked based on the difference in AIC relative to the exponential waning model with sigmoidal booster uptake (ΔAIC). The next best performing model was the leaky model, with $\Delta\text{AIC} = 10.9$. Compared with the waning model, we estimated a higher value of R_0 for the leaky hypothesis (22; 95% CI: 21, 24). This model explains the mumps resurgence in the early 2000s as a result of the introduction of a new genotype in 2000 that caused the erosion of herd immunity. Due to the limited size of the outbreak relative to prevaccination levels, our estimates of vaccine leakiness were highly constrained, $\varepsilon = 3\%$ (95% CI: 2.9%, 3.1%). Consequently, the leaky model predicts that the vaccine retained a high population-level vaccine impact, $\xi = 96.6\%$ (95% CI: 96.5%, 96.6%). Crucially, while the leaky hypothesis correctly predicts disease resurgence from 2006 onward, the predicted age profile of cases lacks the peak in 15- to 25-y-old individuals found in recent data. Instead, cases are more evenly distributed across age groups (*SI Appendix*, Figs. S7 and S8). The remaining two models (Erlang waning and no loss) both performed substantially worse with $\Delta\text{AIC} = 26.9$ and 207.3, respectively.

The Waning Model Provides a Good Explanation of Recent Mumps Epidemiology. In addition to having the lowest AIC score, time series simulated from the exponential waning model are able to reproduce key epidemiological features of mumps data, including 1) the initial vaccine era decline, 2) a resurgence in the 1980s, and 3) a second resurgence in the mid-2000s (Fig. 2*A*). Two dynamical features that this model struggles to capture are 1) the peak and duration of the mid-80s reemergence and 2) the distinct outbreaks in 2006 and 2010, which the model combines into a single multiyear outbreak. Predictive accuracy was limited during the first reemergence era (Fig. 2*A*). This was likely due to overdispersion in the reporting errors as suggested by our parameter estimates (*SI Appendix*, Fig. S9*C*). To validate our fitted model, we withheld the final five years of the time series (2013 to 2018). Strikingly, our model accurately captures the multiannual dynamic signature and correctly predicts the epidemic in 2017.

We quantified the predictive performance of the exponential waning model using the coefficient of determination (R^2). To isolate predictive characters of the model across the six age-specific time series, we estimated R^2 independently for each age cohort (Fig. 2*B*). We found that the model best captures the dynamics associated with the unstructured cases (those with missing age information) ($R^2 = 93\%$). We observed the lowest R^2 in the [25, 40) y age cohort where the model explained 39% of observed variation. In other age classes, we report relatively high values of R^2, we report relatively high values of R^2 with 67%, 77%, 59%, and 41% for [0,5) y, [5,15) y, [15,25) y, and >40 y respectively. Surprisingly, for the majority of age groups, the prediction in the out-of-sample epoch outperforms the prediction in the training data (Fig. 2*B*). This improved performance is less surprising than it may at first appear and is probably an artifact of the small out-of-fit sample (*SI Appendix*, Fig. S6).

In addition to exploring the performance of the model at recapitulating the time series for each individual age group, we also examined how well our model captures the age profile of cases. A salient recurring feature common to the majority of the recent epidemics is the upward shift in the mean age of infection in the reported cases relative to the prevaccine or early vaccination era (38, 44, 45). We find that our model accurately tracks observed trends in the mean age of infection calculated (Fig. 3*A*). To further explore how well our fitted model reproduces the full age distribution of cases, we compared the dynamics of the estimated true age distribution to the model simulated age distribution (Fig. 3*B*). The waning model was able to reproduce the dynamics in the age distribution with strikingly good overall accuracy. To quantify relative agreement between the observed and the expected age distributions, we calculated the Kullback–Leibler Divergence ($\overline{D}^{KL}$, Fig. 3*C*). We observed an increase in the bootstrap variance of the $\overline{D}^{KL}$ over time, which we ascribe to two factors: a secular increase in years when incidence was declining (approximately 1992 to 2005; likely due to the increased impact of demographic stochasticity during eras of low prevalence) and then punctuated increases (likely determined by factors not captured by the model, e.g., individual outbreaks which affected specific subpopulations).

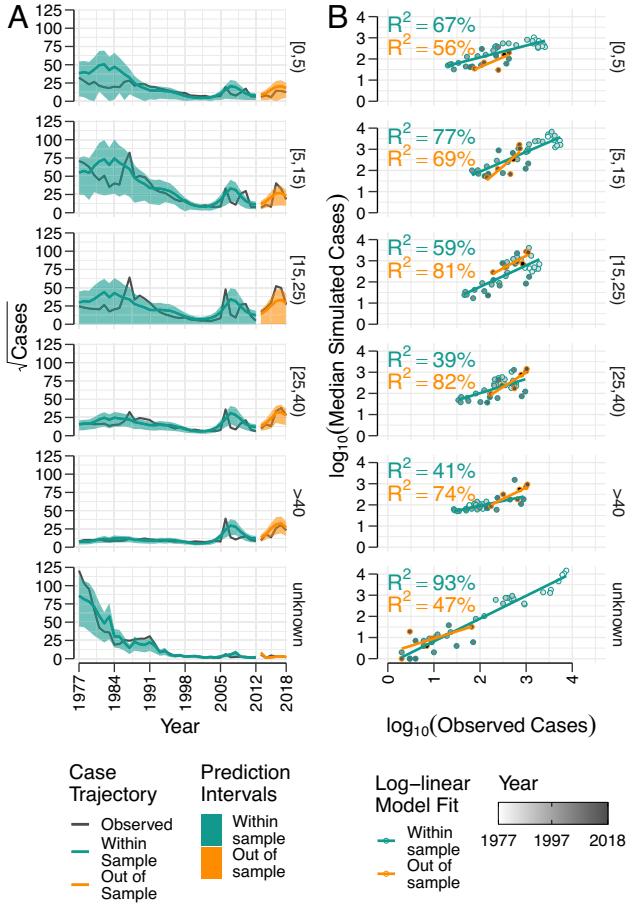

Fig. 2. Model-data agreement. (*A*) Age-specific qualitative model fits to within-sample time series (1977 to 2012, seagreen) and the corresponding 5-y out-of-sample prediction (2013 to 2018, orange) for the waning hypothesis. Ribbons represent 80% prediction intervals for the two prediction epochs. (*B*) Age-specific log-linear model agreement for within-sample fit (seagreen lines and hollow circles) and out-of-sample predictions (orange lines and hollow circles). Statistical performance of the model was assessed using the coefficient of variation (R^2, reported inset) for the two prediction epochs. Year of record is represented using a continuous gray gradient.

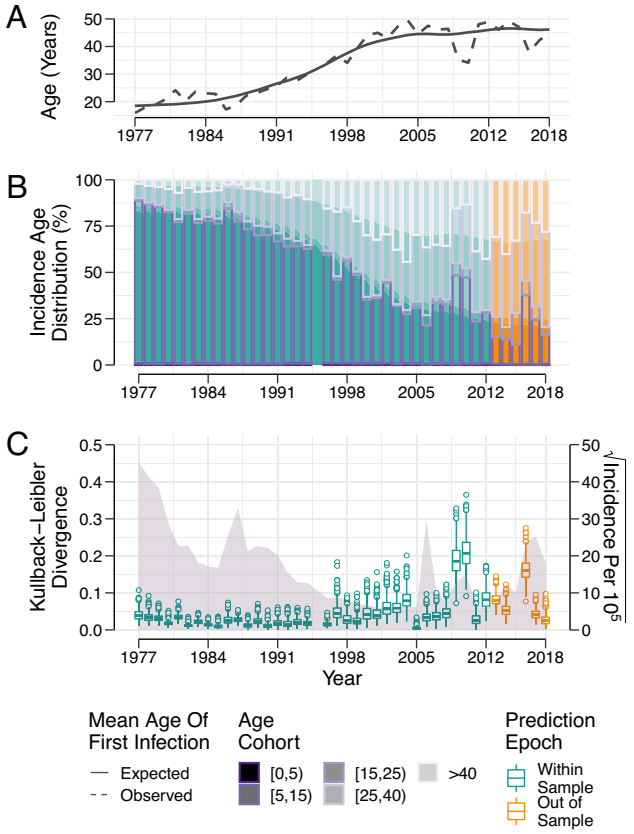

Fig. 3. Relative age distribution of mumps true incidence. (*A*) Expected temporal shifts in the mean age of first infection under the waning model (dotted) relative to the observed incidence (dashed). (*B*) Qualitative comparison between expected incidence, assuming the model of waning immunity, and the observed incidence per 10^5 age distribution (purple gradient). Simulated incidence distribution is broken down into the two prediction epochs—within sample (seagreen) and out of sample (orange)—to match the analysis presented in Fig. 2. Age classes are represented using the gradients of the corresponding colors and are represented as gray in the legend. (*C*) Quantitative agreement between the observed and expected age distribution of incidence using the Kullback–Leibler divergence (KLD, *Left* y-axis) through time. Boxplots represent bootstrapped distribution of KLD calculated by comparing observed age distribution to 1,000 synthetically generated time series under the estimated observation noise. The area plot represents an estimate of age-aggregated mumps incidence per 10^5 (*Right*, y-axis).

Long-Term Trends in Population Immunity Explain the US Mumps Resurgence. The results of our statistical inference allow us to reconstruct changes in the immune profile of the US population after the introduction of vaccines (Fig. 4). Using the fitted model, we estimated a long average duration of vaccine-derived immune protection of 111 y (95% CI: 93 y, 144 y). While this is longer than the typical human lifespan, our results favor an exponential distribution for the duration of immunity. Consequently, an average duration of 111 y implies that 80% of individuals remain immune for at least 20 y after their last dose and that less than 50% remain immune after 80 y. Importantly, our results show that herd immunity is not possible using the existing vaccine, as the fraction of vaccinated individuals who remain immune drops below 93% (the approximate herd immunity threshold calculated via $1 - 1/R_0$) within 8 y of the last administered vaccine dose. These findings clearly identify a role for age-specific boosting schemes.

By incorporating vaccine uptake and demographic data, our model is also able to reconstruct the proportion of the population with vaccine immune protection by age cohort through time (Fig. 4*B*) and the number of individuals who lose immunity each week (Fig. 4*E*). Our results suggest that the proportion of the US population over 25 y who are susceptible to mumps (composed of individuals whose immunity has waned or have not received the full two-dose schedule vaccine) has gradually risen over time reaching around 16% by 2,000 (Fig. 4*D*). From our reconstructed susceptible profile, we can calculate the effective reproductive number over time (Fig. 4*C*), finding that the effective reproductive number remained just above 1 (characteristic of an endemic disease) until the 1985 resurgence, after which it remained below 1 until the late 90s when it entered an oscillatory phase driven by susceptible build-up punctuated by recurrent outbreaks (Fig. 4*F*).

Sensitivity of the Relative Prevalence to the Duration of Immunity. To evaluate the sensitivity of our results, we performed a simulation study to investigate how the frequency of breakthrough infections relative to naive infections is affected by the duration of vaccine protection. Due to the difficulty in interpreting the average immune duration when it is exponentially distributed, we instead quantify vaccine protection in terms of the proportion of the vaccinated population who have lost immunity

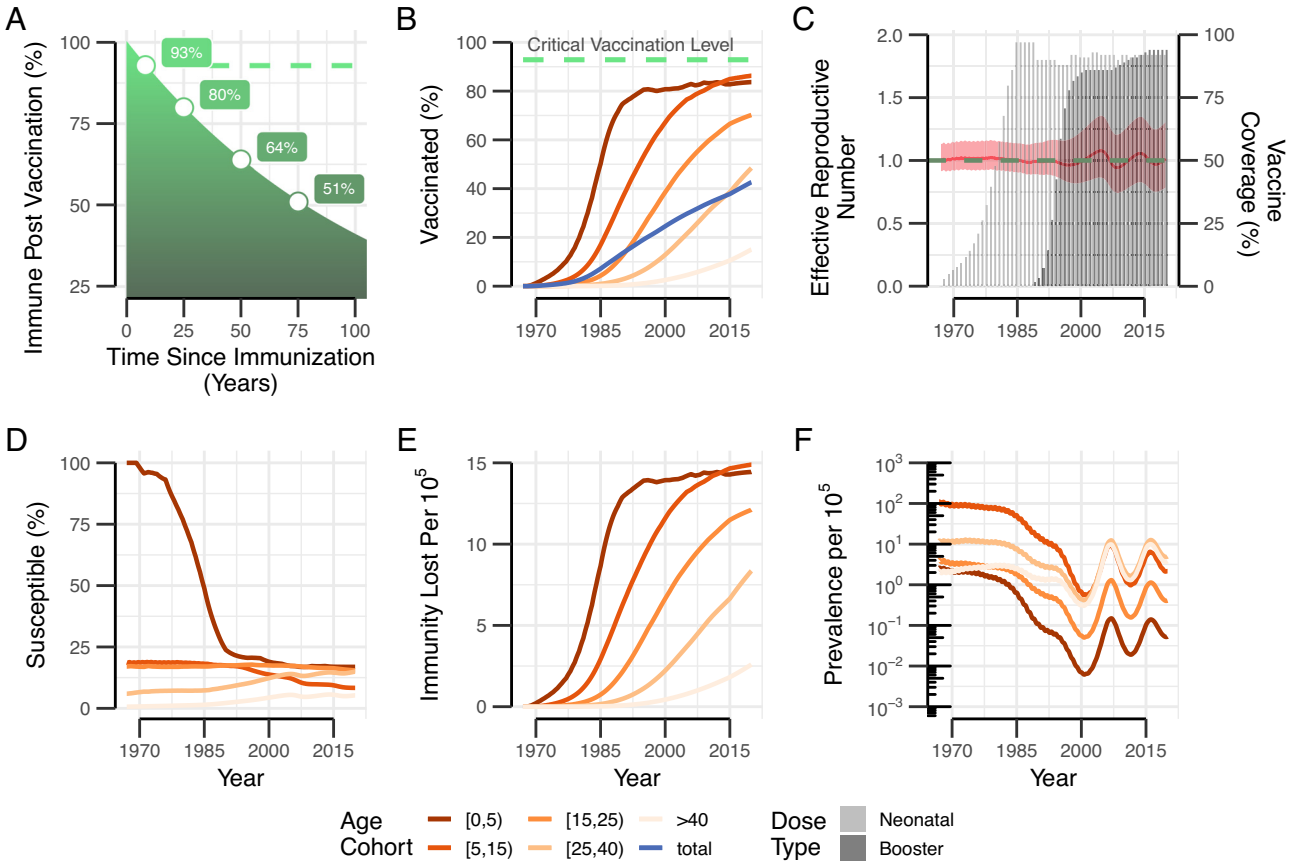

Fig. 4. Reconstructed population immune profile and impact on mumps resurgence. (*A*) Proportion of vaccinated individuals retaining immunity over time for the exponential waning. The average duration of immunity was fixed to $1/\delta = 111.5$ y (i.e., the maximum likelihood estimate). The green dashed line indicates the approximate critical vaccination level for the exponential waning model. Here, the critical vaccination threshold was approximated using $1 - 1/R_0$. (*B*) Percent of the population with vaccine immune protection by age cohorts over time. (*C*) Dynamics in the effective reproductive number highlighting epidemic transitions between supercritical and subcritical (red solid) with 95% confidence intervals (red ribbons) (*Left*, y-axis). Annual vaccination rates of neonatal (light gray) and booster (dark gray) doses (*Right*, y-axis). (*D*) Time series of age-specific susceptibility profiles. (*E*) Number of individuals who lose immunity each week per 10^5. (*F*) Weekly mumps prevalence per 10^5 individuals in each age cohort ($10^5 * I_a/N_a$).

by age 18 y, which we denote P_{18}. Complementing the results shown in Fig. 4*A*, we find that P_{18} exceeds 6% even when the average immune duration is 200 y.

Our model allowed us to assess the impact of waning immunity on the individual level and quantify the ratio of infections in individuals whose vaccine immunity has waned (I_W) to those in unvaccinated individuals (including nonvaccinated and those with primary vaccine failure) (I_S), which we refer to as the relative prevalence ratio (RPR). We calculate the RPR separately for each age cohort based on the time since the last vaccine dose received by vaccinated individuals.

Apart from the [0, 5) cohort, the RPR was always greater than 1, implying more infections in previously vaccinated individuals than the unvaccinated (Fig. 5*A*). For the younger age groups ([0, 5) y and [5, 15) y), increasing the average duration of immunity (i.e., decreasing P_{18}) always resulted in a drop in the RPR. For long-lasting immunity, there was a general trend that as the population aged, RPR rose due to waning immunity providing a mechanism for susceptible recruitment unavailable to the unvaccinated compartment. Interestingly, unlike in the case of the younger age classes, we observed a nonmonotonic effect of waning intensity on the RPR of the older age groups (>15 y). For these older age cohorts, under a rapid waning scenario, the RPR was comparable to a low waning intensity. This, we posit, is a consequence of contesting flows of waning and aging among the individuals in the population. For the scenario with long-lasting immunity (Fig. 5*A*, purple region), most of the vaccinated individuals remained protected against infection during their life time. Conversely, with a vaccine-derived immunity that was short-lived (Fig. 5*A*, orange region), individuals rapidly lost protection and were soon infected. The aging in relation to the transmission process in this scenario occurs at a substantially lower rate. Susceptible individuals who have lost their immunity become infected and have recovered from the infection by the time they graduate from an age class. This effect was exacerbated with the wider age cohorts, generating a greater overlap of the RPR for a vaccine with longer immune duration compared with a scenario where the immunity wanes rapidly. Highest values of RPR for these older age classes were therefore produced at intermediate values of immune loss probability. This phenomenon has also been documented in the case of other disease systems like pertussis (35) and in the recent and ongoing pandemic of the novel SARS-CoV-2 (46).

It is important to note that since we are considering the ratio of I_W/I_S, and not taking into account the fraction of the population who received the vaccine, the RPR can exceed 1, indicating that more infections are taking place in individuals whose immunity has waned than were unvaccinated. Indeed, the RPR for $P_{18} = 1$ (which corresponds to a completely ineffective vaccine) reflects the vaccine uptake.

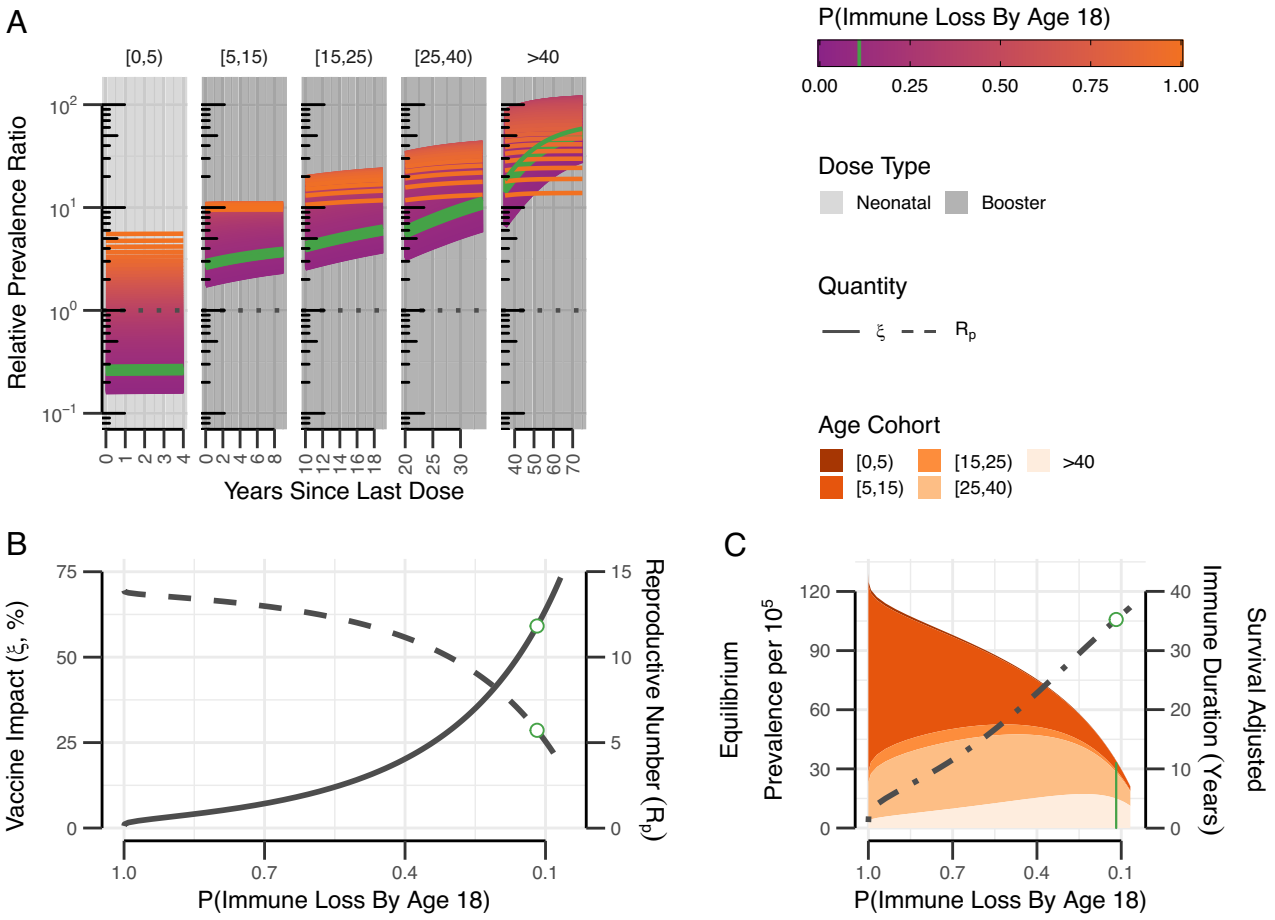

Fig. 5. Age-specific immunity post vaccination (*A*) Relative prevalence ratio ($I_i^w(t)/I_i^s(t)$) of infection after vaccination across the five age cohorts (facet columns), as a function of varying probability of immunity loss by the age of 18 y (color gradient). Estimated MLE of immune duration was converted to probability of immune loss (indigo); time underwent a reset to 0 y after administration of neonatal dose (gray background) and booster dose (black background). (*B*) Population-level vaccine impact (solid lines) and reproductive number (dashed lines) calculated at 91.7% and 91.6% neonatal and booster vaccine coverage respectively (fixed at an average for 2008 to 2018) as a response and (*C*) stable-state prevalence distribution across five age cohorts as a function of varying probability of immune loss by age 18 y. Relationship between survival-adjusted duration of immunity (*SI Appendix*, section A.8) and probability of immune loss by age 18 y are represented on the secondary axis (dot-dashed lines). Covariate values were fixed at the last known value in the year 2018. Dynamics were simulated for 300 y, and final values in the infectious compartments values were taken to be prevalence per 10^5.

Clinically, the observation of infections predominantly among previously vaccinated individuals can be misconstrued to imply that vaccines are ineffective at controlling transmissible pathogens. To rebut this claim, we calculated the population-level vaccine impact as a function of varying waning intensities. Overall, we observed that a decrease in the waning intensity substantially decreases infection prevalence (Fig. 5*C*), confirming that vaccines which impart long-lasting immunity are indeed impactful in the control of pathogens like mumps, and that having a larger proportion of infections represented in the vaccinated subpopulation is merely an expected artifact of the waning immunity at a population level. For our system, however, we estimated a relatively modest vaccine impact (59.1%) at the population level. We speculate that this might be a joint outcome of high viral transmissibility ($R_0 = 14$) and a substantial primary vaccine failure probability ($\alpha = 0.054$).

Discussion

The recent reemergence and continued persistence of mumps in countries with high estimated vaccine coverage has been perplexing, casting doubt on global health goals (47). A major obstacle in this context is the absence of serological correlates of protection against mumps. Indeed, it still remains unclear what components of the host immune system are adaptively immunogenic against subsequent infections and what constitutes an infectious dose for a successful transmission event for entry and establishment of an infection (48).

In the absence of straightforward immunological indicators of protection, we attempted to disentangle the putative mechanisms underlying the reemergence of mumps in the United States by statistically contending compartmental models describing mechanisms for vaccine failure and their effect on the circulation of the mumps virus. Among the models contested, we found that the exponential waning model is most consistent with the observed data.

Importantly, our exponential waning model reconciles population-level immunological trends with seemingly contradictory individual-level clinical observations. Specifically, while a long average immune duration of immunity is estimated and around 50% of individuals retain immunity for their entire lives, we estimate that 11.77% (95% CI: 0.1%, 11.81%) of vaccinated individuals lose immunity by the age of 18 y. Given persistent high coverage, this explains the paradoxical clinical observation that most infections occur in vaccinated individuals. Furthermore, our results explain the resurgent dynamics and the

shift in the age profile of cases. As the immune profile shifts from being mostly due to natural infection (which we take to be lifelong, consistent with a lack of documented reinfections) to vaccine-derived, the impact of waning immunity rises. This leads to a growing pool of older susceptible individuals with waned vaccinal immunity (who in the prevaccine era would likely have natural immunity) among which the virus can spread. Such multidecadal trends can result in the initial achievement of herd immunity (when only younger individuals have received vaccines and most older individuals possess natural immunity) before it is lost (as the vaccinated individuals age and their immunity wanes).

We found that the leaky scenario is not consistent with the available epidemiological data. While a small but nonzero leakiness parameter was able to generate outbreaks matching the timing and size of post-2006 resurgence, our results show that if leakiness is the mechanism of reemergence, then the rise in incidence should be approximately uniformly realized across all age classes. Assuming a constant contact structure and an imported genotype with transmissibility identical to the previously circulating genetic variant, these dynamics should stabilize to the prevaccine age distribution of cases. Instead, we documented a gradual increase in the mean age of first infection in the observed mumps dynamics. This pattern is consistent with the waning hypothesis. The limited spread and the age profile of cases during recent resurgences place constraints on the possible role of immune mismatch.

Although our exponential waning model successfully explains the long-term trends in mumps epidemiology in the United States, it fails to capture some of the finer, temporally resolved characteristics of the data in the two resurgence eras (1985 to 1989 and 2000 to 2012). Particularly, the average simulated dynamics 1) underestimate the peak and overestimate the duration of the mid-80s reemergence and 2) they combine outbreaks in 2006 and 2010 into a single multiyear outbreak. In both scenarios, we believe that model-data disagreements are the result of spatial heterogeneity and stochasticity in the disease transmission process when incidence is very low (49), which our deterministic and spatially aggregated model is not designed to capture. In both the resurgent eras (1985 to 1989 and 2006 to 2012), mumps incidence in mid-western states surrounding Illinois and Iowa, respectively, contribute disproportionately to overall cases observed (Fig. 1 *D* and *E*). Another model limitation is our parsimonious assumption that vaccine leakiness (i.e., the probability that a mismatched virus can infect a vaccinated individual) does not depend on age. Given that the leaky model is outperformed by the exponential waning model, it would be interesting to examine whether its performance improves if the impact of immune evasion depends on either age or the time since the last vaccine dose.

Our findings are consistent with those presented in two recent studies exploring drivers of reemergence of mumps in the United States during the vaccine era. The phylogenetic analysis of Wohl et al. (19) found no evidence in support of immune evasion among the mumps genotypes that dominate circulation in the northern US and concluded that waning vaccine immunity is the plausible explanation for mumps resurgence. The study by Lewnard and Grad successfully reproduced the age distribution of observed cases in the 2006 mumps epidemic using a model of waning efficacy fitted to vaccine trial data (18). Their meta-analysis of estimates from vaccine efficacy trials arrived at a mean duration of immunity of 27.4 y (95% CI, 16.7 to 51.1 y). To compare directly their estimated duration of immunity with our fitted estimate, we need to calculate the expected time to loss of immunity (T_L) conditioned on the survival of an individual (i.e., $T_L < T_D$, where T_D is the time to death). As we show in *SI Appendix*, section A.8, assuming a constant lifespan of duration τ, this quantity is given by

$$\mathbb{E}[T_L | T_L < T_D] = \frac{1}{\delta} - \frac{\tau e^{-\delta\tau}}{1 - e^{-\delta\tau}}. \quad [1]$$

Given our estimate of $\delta = 1/111.5\ \mathrm{y}^{-1}$ and assumed lifespan $\tau = 80$ y, we find that $\mathbb{E}[T_L | T_L < T_D] \approx 35.3$ y, consistent with the estimate of Lewnard and Grad. Thus, by doing the careful book-keeping of susceptible recruitment dynamics at the national level, we arrive at a similar conclusion to prior studies. Our results bolster the confidence that the waning hypothesis is indeed the most plausible driver of the ongoing resurgence of mumps. Our study, like the previous ones, supports in principle, the roll-out of a third booster dose of the mumps vaccine (50, 51) and suggests the utility of periodic targeted immune boosting of immunity among college going adults (52).

For computational reasons, we excluded the effects of demographic stochasticity from our analysis. Models that include these effects have demonstrated improved statistical performance (35, 53) and can shrink nonsystematic prediction errors (54). However, to justify the use of a mean-field model in this analysis, we performed a simulation study to verify the sensitivity of point estimates to effects of demographic stochasticity. We found comparable fits and parameter MLEs of a deterministic model when fit to synthetic time series simulated with and without the inclusion of process noise (*SI Appendix*, Fig. S10 and Table S5). In addition, our analyses of incidence records relied on point-value estimates for two parameters from the literature, namely the mean infectious period and the primary vaccine failure probability. Both parameters are fairly well constrained by previous studies e.g., the primary vaccine failure probability is estimated to be 0.066, 95% CI:(0.046-0.092) (55), and we do not expect the values used to drastically alter our conclusions. That said, the use of point estimates can also inflate confidence in statistical analyses (see e.g., ref. 56), and propagating the uncertainty in these parameters (e.g., by using a Bayesian analysis) might produce more reliable confidence intervals.

In summary, our analyses indicate that waning immunity provides a parsimonious explanation for the resurgence of mumps in the United States. We found that, due to the combination of waning immunity and primary vaccine failure, robust herd immunity cannot be achieved with the present vaccine and immunization schedule. Indeed, our results support, in principle, the administration of regular booster doses to achieve and maintain herd immunity. An area of priority for future research is the use of empirically validated models such as ours to identify economically cost-effective and epidemiologically efficient age-targeted vaccination schemes with the view to control and eventually eliminate mumps circulation in the United States.

Materials and Methods

Case Reports and Covariate Data. We acquired mumps incidence data from two separate sources. Annual tables on the age-specific case reports of mumps were acquired from the Morbidity and Mortality Weekly Reports (MMWR) published by the Centers of Disease Control (CDC) (38). Initially, MMWR pdf tables were digitized to a computer-readable format. Further, the age-specific case reports were aggregated to generate six time series with uniform widths during 1977 to 2018 (Fig. 1 *A*–*C*). Weekly aggregated case reports were

downloaded from the Project Tycho database (39). These data were spatially grouped to generate a high-frequency time series of national-level mumps case reports during 1967 to 1985 (*SI Appendix*, Fig. S2*B*). We temporally aggregated data from the weekly time series to generate the average spatial distribution of mumps in the United States during the two major epidemics in the vaccine era (Fig. 1 *D* and *E*).

Data on demographic covariates were downloaded from the US census website (57). We processed the demographic time series to generate 1) age-specific estimates of national-level population sizes consistent with the age groupings of the reported mumps cases, 2) estimates of age-specific migration rates (*SI Appendix* for details Fig. 1 *A*–*C*), and 3) national-level estimates of the annual birth rates for the United States (*SI Appendix*, Fig. S3 *B*, *D*, and *E*). To account for the associative mixing among the various age-based subpopulations, we used the contact matrix reported in the POLYMOD study (58) for the United Kingdom. This allowed us to include a social contact structure that is closely comparable to the United States in our analysis. This contact matrix was transformed to correct for reciprocity, such that the total daily contact rates had a symmetric structure, and to match age distribution for the United States (*SI Appendix*, Fig. S1, for details). National-level coverage estimates of mumps vaccines, for the neonatal and booster schedule, were downloaded from the World Health Organization (WHO) website (59). Ideally, the estimates on vaccine rates would have been extracted from the MMWR. However, coverage data during the last two decades as reported by the MMWR are incomplete with several years of missing records. Moreover, unlike WHO, MMWR does not explicitly publish neonatal and booster dose coverage. The two data sources however were in good agreement with one another (*SI Appendix*, Fig. S11). Thus, vaccine coverage as reported by WHO was used in this analysis. Finally, missing early coverage for these time series was interpolated for both doses (*SI Appendix*, Fig. S2 *C* and *D*; for details).

Models of Mumps Reemergence. To investigate the potential mechanism of vaccine failure in explaining the reemergence of the mumps virus, we formulated an age-structured Susceptible-Exposed-Infectious-Recovered (*SEIR*) transmission model (49). The population, with total size $N(t)$, was divided into six compartments. Individuals enter the first vaccinated compartment (V^1) at the rate $(1-\alpha)p(t)\nu(t)$, where $p(t)$ is the annual infant immunization coverage in the year t, α is the probability of primary vaccine failure, and $\nu(t)$ is the per capita birth rate. The remainder of the newborns are assumed to be susceptible (S) who can become infected with either mumps genotypes at rate λ_n, where λ_n is the force of infection of mumps genotype n ($n \in \{A, G\}$). Following infection, individuals move into the corresponding exposed compartments, E^n, remaining latently infected for a period of $\frac{1}{\sigma}$ days before moving to the infectious compartments, I^n. Ultimately, the infection is cleared following a mean duration of $\frac{1}{\gamma}$ days, and individuals acquire long-term immunity, as they enter the recovered (R) compartment. Vaccine-derived immune protection in this system lasts for a total duration of $1/\delta$ years after which individuals reenter the S class (Eqs. **3**–**6**). Here, we considered a model with variable (specifically 1, 2, and 3) subclasses for the vaccinated subpopulation in order to generate a gamma-distributed waiting time with shape parameter x (49, 60, 61). When $x = 1$, we recover the exponential distribution, and as x increases, the distribution becomes increasing peaked about $(1/\delta)$ with the variance declining according to $\frac{1}{x\delta^2}$. Vaccinated individuals are also capable of acquiring the infection with a force of infection reduced by a genotype-specific factor ε^n, which is typically referred to as the vaccine leakiness (29, 43). The model accounts for the importations of infectious individuals of genotype n at the rate ι^n per year. *SI Appendix*, Fig. S4 describes the vaccine imperfection model skeleton.

The genotype-specific force of infection is proportional to the number of individuals in the I^n compartment and the seasonality of transmission,

$$\lambda^n(t) = qC\left[1-\beta_1|DG\sin\left(\frac{2\pi t}{T}\right)\right]\frac{I^n(t)}{N(t)}. \quad [2]$$

Here, q, C, and β_1 are the probability of infection given contact, the average daily contact rate, and the amplitude of seasonality respectively, and T is the period of seasonality (assumed to be 1 y). The model dynamics are represented using the following system of differential equations

$$\frac{dS}{dt} = \left(1-(1-\alpha)p(t)\right)\nu(t)N(t) + 3\delta V^3 - \left(\sum_n \lambda^n(t) + \mu(t)\right)S, \quad [3]$$

$$\frac{dV^1}{dt} = (1-\alpha)p(t)\nu(t)N(t) - \left(3\delta + \sum_n \varepsilon^n\lambda^n + \mu(t)\right)V^1, \quad [4]$$

$$\frac{dV^2}{dt} = 3\delta V^1 - \left(3\delta + \sum_n \varepsilon^n\lambda^n + \mu(t)\right)V^2, \quad [5]$$

$$\frac{dV^3}{dt} = 3\delta V^2 - \left(3\delta + \sum_n \varepsilon^n\lambda^n + \mu(t)\right)V^3, \quad [6]$$

$$\frac{dE^n}{dt} = \lambda^n(t)\left(S + \varepsilon^n V\right) - \left(\sigma + \mu(t)\right)E^n + \iota^n, \quad [7]$$

$$\frac{dI^n}{dt} = \sigma E^n - \left(\gamma + \mu(t)\right)I^n, \quad [8]$$

$$\frac{dR}{dt} = \gamma\sum_n I^n - \mu(t)R. \quad [9]$$

Here, $\varepsilon_n = \varepsilon$ when $n = G$, and 0 otherwise; $\iota^n = \iota$ when $n = G$ and $t = t_{intro}$, 0 otherwise. The aforementioned model (Eqs. **3**–**9**) distills the essential reactions representing various imperfection traits. For complete details on the full age-structured model, compartments, and parameter definitions and *SI Appendix*, Tables S1 and S2.

For statistical inference with the case data, we kept track of new cases generated by the model. This was achieved by calculating a piece-wise integral over a time period equal to the observed data (1 y), with the expression for new cases over the annual interval $[t-1, t)$ given by

$$C_t = \int_{t-1}^{t} \gamma\sum_n I^n(s)ds. \quad [10]$$

The model was implemented in R package "pomp" (62).

Reproductive Numbers and Vaccine Impact. We derived an expression for the basic reproductive number (R_0) for the age-structured transmission model using the next-generation method (NGM) (63) (*SI Appendix* for details). As R_0 quantifies pathogen transmissibility in a fully susceptible population (i.e., without vaccination), we derived an analogous measure of transmissibility in the presence of the vaccine, which we denote R_p. Using these two reproductive numbers, we further derived an expression for the population-level vaccine impact, ξ, defined as the decrease of transmissibility of the virus in the presence of the vaccine ($P > 0$) relative to the transmission in absence of the vaccine ($P = 0$) (43),

$$\xi = 1 - \frac{R_p}{R_0}. \quad [11]$$

Parameter Estimation and Hypothesis Testing. We used age-stratified time series of annual mumps case reports (Fig. 1*B*) to perform maximum-likelihood estimation of model parameters to ascertain relative support among five qualitatively distinct hypotheses. These were as follows: 1) The "no loss" hypothesis assumes that the vaccine is perfect ($\varepsilon = 0$, $\delta = 0$); 2) the "exponential waning" hypothesis assumes that the vaccine-derived immune protection wanes over time with exponentially distributed duration and that there

is no vaccine leakiness ($\varepsilon = 0$); 3) the "Erlang waning" hypothesis is the same as the exponential waning hypothesis but assumes that the duration of immunity is Erlang-distributed with shape parameter $x = 2$; 4) similarly, an Erlang-distributed immune duration model with shape parameter $x = 3$ (see above); 5) the "leaky" hypothesis assumes that at time $t = t_{intro}$, a novel genotype is introduced to the population against which the vaccine provides leaky immunity ($\varepsilon > 0$). For the leaky hypothesis, we also analyzed the impact of introducing the novel genotype to differing age classes. Moreover, for each hypothesis, we also investigated the effect of four different shapes of booster uptake immediately following its roll-out. A formal comparison of all these models was conducted as described below.

Trajectory matching was employed to find maximum-likelihood estimates of the unknown model parameters. As the data included cases without recorded age ("unstructured cases") as well as age-structured cases, we constructed a reporting model capable of fitting to both data types by including a time-varying probability of age being recorded, η_t, calculated from the proportion of case reports that were age-structured (*SI Appendix*, Fig. S3*A*). We assumed that the observation errors in both age-structured and unstructured annual case data followed a normal distribution allowing for overdispersion in the reporting process (64). Specifically, for age-structured data, the mean and variance in the number of reported cases at time t in age group i that depend on the age-specific reporting probability, ρ_i, and overdispersion parameter, ψ_i, are given by

$$\mu_{i,t} = \rho_i \eta_t C_{i,t}, \quad [12]$$

$$\sigma^2_{i,t} = \mu_{i,t}(1 - \rho_i \eta_t + \psi_i^2 C_{i,t}), \quad [13]$$

for $i \in \{[0, 5), [5, 15), [15, 25), [25, 40), \geq 40\}$. The unstructured data are distributed similarly, with mean and variance

$$\mu_{u,t} = \rho_u (1 - \eta_t) \sum_i C_{i,t}, \quad [14]$$

$$\sigma^2_{u,t} = \mu_{u,t} \left(1 - \rho_u (1 - \eta_t) + \psi_u^2 \sum_i C_{i,t} \right), \quad [15]$$

where ρ_u and ψ_u are the reporting probability and overdispersion parameter for unstructured cases. The likelihood function for the observed age-structured data $D_{i,t}$ and unstructured data $D_{u,t}$, conditioned on the model parameter vector Θ, was given as

$$\mathcal{L}(\Theta) = \prod_t \left(f\left(D_{u,t}; \mu_{u,t}, \sigma^2_{u,t}\right) \prod_i f\left(D_{i,t}; \mu_{i,t}, \sigma^2_{i,t}\right) \right), \quad [16]$$

where $f\left(x; \mu, \sigma^2\right)$ is the probability density function of a normally distributed random variable with mean μ and variance σ^2.

Maximization of the likelihood function (Eq. **16**) was carried out using a differential evolutionary (DE) algorithm. It is a stochastic optimization approach that is known to provide an efficient convergence to the global optimum for real-valued objective functions (*SI Appendix* for details). DE was implemented using the R package DEoptim (65). The latent state variables were initialized near an endemic equilibrium. The first 100 y were discarded as transient dynamics, and subsequent 36 y (1977 to 2012) were used in the calculation of likelihood. To compare the relative goodness of fit among the four competing hypotheses, we used the Akaike information criterion (AIC), defined as

$$AIC = 2p - 2log\left(\mathcal{L}(\Theta)\right), \quad [17]$$

where p is the number of free model parameters. Confidence intervals on parameter estimates at a 5% level of significance were calculated for each of the four models using a likelihood-ratio test (equivalent in this instance to finding regions of parameter space with an AIC within 1.92 of the minimum for the given model).

Uncertainty Estimation. We used parametric bootstrapping to estimate confidence intervals for MLEs. This involved the following: 1) For each model, MLEs obtained in the preceding section were used to simulate 5,000 synthetic time series. 2) Starting at the MLE, a local search with a Nelder–Mead optimizer (66) was conducted and the parameters estimated for every time series. 3) This results in a bootstrapped distribution of parameter estimates. Estimate sets corresponding to 2.5th and 97.5th percentiles of this distribution were taken to be as the 95% confidence bounds of the model MLEs.

Model Performance. A subset of the case-reports data (6 y, 2013 to 2018) was reserved to test the performance of the model by conducting out-of-sample prediction. Model performance was quantified using the coefficient of determination (67), R^2, between the observed case records (D) and the log-transformed median simulated reported cases (M),

$$R^2 = \left[\frac{CoV(D, M)}{\sqrt{V(D)V(M)}} \right]^2, \quad [18]$$

where $CoV(D, M)$, $V(D)$, and $V(M)$ are covariance between D and M, variance of D, and variance of M, respectively. We computed values of R^2 for each separate age group during both the within-sample (pre-2013) and out-of-sample infection prediction epochs.

We also compared how the resulting age distribution of the observed case data compared with the simulated cases from the best fitting model using the Kullback–Leibler divergence (68). For this analysis, we ignored the unstructured subset of reported cases due to their diminishing presence in the recent epidemics (Fig. 1*B*). Age distributions for observed and simulated cases were constructed by normalizing the data for each week, i.e., $A^D_{i,t} = D_{i,t} / \sum_i D_{i,t}$ and $A^M_{i,t} = M_{i,t} / \sum_i M_{i,t}$. The Kullback–Leibler divergence for each time point was then given by

$$\overline{D}^{KL}_t = \frac{1}{2} \left[\sum_i A^D_{i,t} log\left(\frac{A^D_{i,t}}{A^M_{i,t}} \right) + \sum_i A^M_{i,t} log\left(\frac{A^M_{i,t}}{A^D_{i,t}} \right) \right]. \quad [19]$$

We quantified uncertainty in our estimate of $\overline{D}^{KL}_t$ using bootstrap sampling. We sampled 1,000 simulated replicates from our reporting model and calculated $\overline{D}^{KL}_t$ for each replicate by replacing $A^D_{i,t}$ in Eq. **19** with the simulated data.

Data, Materials, and Software Availability. Source code and data underlying this article are available in the zenodo repository https://doi.org/10.5281/zenodo.7434784, and can be accessed with the url https://doi.org/10.5281/zenodo.7434784.

ACKNOWLEDGMENTS. This project has been funded in part with Federal funds from the National Institute of Allergy and Infectious Diseases, NIH, Contract No. 75N93021C00018 (NIAID Centers of Excellence for Influenza Research and Response, CEIRR) and from the NSF under Grant No. DGE-1545433 (IDEAS training program). TSB acknowledges support from the National Institute Of General Medical Sciences of the NIH under Award Number R01GM123007. We would like to thank Dr. Ben Bolker and the anonymous reviewer for their astute critique of this study. We would also like to thank Dr. Arash Seidpour for his input on the analysis presented in this study.

Author affiliations: [a]Odum School of Ecology, University of Georgia, Athens, GA 30602; [b]Center of Ecology of Infectious Diseases, Athens, GA 30602; [c]Center for Influenza Disease & Emergence Research, Athens, GA 30602; [d]Department of Infectious Diseases, College of Veterinary Medicine, University of Georgia, Athens, GA 30602; [e]Department of Ecology & Evolutionary Biology, University of Michigan, Ann Arbor, MI 48109; and [f]Center for the Study of Complex Systems, University of Michigan, Ann Arbor, MI 48109

1. A. E. Barskey, J. W. Glasser, C. W. LeBaron, Mumps resurgences in the United States: A historical perspective on unexpected elements. *Vaccine* **27**, 6186–6195 (2009).
2. H. Peltola *et al*., Mumps outbreaks in Canada and the United States: Time for new thinking on mumps vaccines. *Clin. Infect. Dis.* **45**, 459–466 (2007).
3. R. K. Gupta, J. Best, E. MacMahon, Mumps and the UK epidemic 2005. *BMJ* **330**, 1132–1135 (2005).
4. H. Jick, D. P. Chamberlin, K. W. Hagberg, The origin and spread of a mumps epidemic: United Kingdom, 2003–2006. *Epidemiology* **20**, 656–661 (2009).
5. S. H. Park, Resurgence of mumps in Korea. *Infect. Chemother.* **47**, 1–11 (2015).
6. G. St-Martin *et al*., Mumps resurgence in Denmark. *J. Clin. Virol.* **61**, 435–438 (2014).
7. G. Dayan, S. Rubin, Mumps outbreaks in vaccinated populations: Are available mumps vaccines effective enough to prevent outbreaks? *Clin. Infect. Dis.* **47**, 1458–1467 (2008).
8. S. Plotkin, W. Offit, P. E. KM, Plotkin's vaccines (2018).
9. J. P. Stahl, A. Mailles, L. Dacheux, P. Morand, Epidemiology of viral encephalitis in 2011. *Med. et Mal. Infect.* **41**, 453–464 (2011).
10. H. Hashimoto, M. Fujioka, H. Kinumaki, K. A. P. S. Group, An office-based prospective study of deafness in mumps. *Pediatr. Infect. Dis. J.* **28**, 173–175 (2009).
11. J. C. Morrison, J. R. Givens, W. L. Wiser, S. A. Fish, Mumps oophoritis: A cause of premature menopause. *Fertil. Steril.* **26**, 655–659 (1975).
12. H. Wu, F. Wang, D. Tang, D. Han, Mumps orchitis: Clinical aspects and mechanisms. *Front. Immunol.* **12**, 848 (2021).
13. Mumps vaccination (2021).
14. P. Mortimer, Mumps prophylaxis in the light of a new test for antibody. *Br. Med. J.* **2**, 1523–1524 (1978).
15. A. M. Galazka, S. E. Robertson, A. Kraigher, Mumps and mumps vaccine: A global review. *Bull. World Health Organ.* **77**, 3 (1999).
16. R. Ramanathan, E. Voigt, R. Kennedy, G. Poland, Knowledge gaps persist and hinder progress in eliminating mumps. *Vaccine* **36**, 3721–3726 (2018).
17. S. Gouma *et al*., Differences in antigenic sites and other functional regions between genotype A and G mumps virus surface proteins. *Sci. Rep.* **8**, 13337 (2018).
18. J. A. Lewnard, Y. H. Grad, Vaccine waning and mumps re-emergence in the United States. *Sci. Trans. Med.* **10**, eaao5945 (2018).
19. S. Wohl *et al*., Combining genomics and epidemiology to track mumps virus transmission in the United States. *PLOS Biol.* **18**, e3000611 (2020).
20. S. Gouma *et al*., Two major mumps genotype G variants dominated recent mumps outbreaks in the Netherlands (2009–2012). *J. General Virol.* **95**, 1074–1082 (2014).
21. S. Vygen *et al*., Waning immunity against mumps in vaccinated young adults, France 2013. *Eurosurveillance* **21**, 30156 (2016).
22. E. J. Homan, R. D. Bremel, Are cases of mumps in vaccinated patients attributable to mismatches in both vaccine T-cell and B-cell epitopes? An immunoinformatic analysis. *Hum. Vaccines Immunother.* **10**, 290–300 (2014).
23. M. A. Riolo, P. Rohani, Combating pertussis resurgence: One booster vaccination schedule does not fit all. *Proc. Natl. Acad. Sci. U.S.A.* **112**, E472–E477 (2015).
24. A. F. Read *et al*., Imperfect vaccination can enhance the transmission of highly virulent pathogens. *PLoS Biol.* **13**, e1002198 (2015).
25. L. Zhou, X. Ge, H. Yang, Porcine reproductive and respiratory syndrome modified live virus vaccine: A "leaky" vaccine with debatable efficacy and safety. *Vaccines* **9**, 362 (2021).
26. M. Łuksza, M. Lässig, A predictive fitness model for influenza. *Nature* **507**, 57–61 (2014).
27. X. Du *et al*., Mapping of H3N2 influenza antigenic evolution in China reveals a strategy for vaccine strain recommendation. *Nat. Commun.* **3** (2019). 10.1038–ncomms1710.
28. S. A. Rubin *et al*., Antibody induced by immunization with the Jeryl Lynn mumps vaccine strain effectively neutralizes a heterologous wild-type mumps virus associated with a large outbreak. *J. Infect. Dis.* **198**, 508–515 (2008).
29. M. E. Halloran, I. M. Longini, C. J. Struchiner, Design and interpretation of vaccine field studies. *Epidemiol. Rev.* **21**, 73–88 (1999).
30. A. R. McLean, S. M. Blower, Imperfect vaccines and herd immunity to HIV. *Proc. R. Soc. London. Ser. B: Biol. Sci.* **253**, 9–13 (1993).
31. M. A. Riolo, A. A. King, P. Rohani, Can vaccine legacy explain the British pertussis resurgence? *Vaccine* **31**, 5903–5908 (2013).
32. L. Jin *et al*., Genomic diversity of mumps virus and global distribution of the 12 genotypes. *Rev. Med. Virol.* **25**, 85–101 (2015).
33. J. Mossong, C. P. Muller, Modelling measles re-emergence as a result of waning of immunity in vaccinated populations. *Vaccine* **21**, 4597–4603 (2003).
34. B. T. Grenfell, O. N. Bjørnstad, B. F. Finkenstädt, Dynamics of measles epidemics: Scaling noise, determinism, and predictability with the TSIR model. *Ecol. Monogr.* **72**, 185–202 (2002).
35. M. Domenech de Cellès, F. M. Magpantay, A. A. King, P. Rohani, The impact of past vaccination coverage and immunity on pertussis resurgence. *Sci. Transl. Med.* **10**, eaaj1748 (2018).
36. R. K. Borchering *et al*., Anomalous influenza seasonality in the United States and the emergence of novel influenza B viruses. *Proc. Natl. Acad. Sci. U.S.A.* **118** (2021).
37. A. A. Al-Dar *et al*., Diphtheria resurgence in Sada'a-Yemen, 2017–2020. *BMC Infect. Dis.* **22**, 1–6 (2022).
38. National notifiable diseases surveillance system (NNDSS) (2018). https://wonder.cdc.gov/nndss.
39. Project tycho (2020). https://www.tycho.pitt.edu/data.
40. J. Hamborsky, A. Kroger, *Epidemiology and Prevention of Vaccine-Preventable Diseases, E-Book: The Pink Book* (Public Health Foundation, 2015).
41. Mumps health care information (2021). https://www.cdc.gov/mumps/hcp.html.
42. R. M. Anderson, R. M. May, *Infectious Diseases of Humans: Dynamics and Control* (Oxford University Press, 1992).
43. F. Magpantay, M. Riolo, M. de Cellés, A. King, P. Rohani, Epidemiological consequences of imperfect vaccines for immunizing infections. *SIAM J. Appl. Math.* **74**, 1810–1830 (2014).
44. PHAo Canada, Government of Canada (2021).
45. R. M. Anderson, R. M. May, Directly transmitted infections diseases: Control by vaccination. *Science* **215**, 1053–1060 (1982).
46. E. Hacisuleyman *et al*., Vaccine breakthrough infections with SARS-CoV-2 variants. *N. Engl. J. Med.* **384**, 2212–2218 (2021).
47. N. MacDonald, T. Hatchette, L. Elkout, S. Sarwal, Mumps is back: Why is mumps eradication not working? Hot topics in infection and immunity in children VII (2011), pp.197–220.
48. Z. M. Shehab, P. A. Brunell, E. Cobb, Epidemiological standardization of a test for susceptibility to mumps. *J. Infect. Dis.* **149**, 810–812 (1984).
49. M. J. Keeling, P. Rohani, *Modeling Infectious Diseases in Humans and Animals* (Princeton University Press (2011). Chapters – 2, 3, 6, 8, pp. 77–92 .
50. M. Kontio, S. Jokinen, M. Paunio, H. Peltola, I. Davidkin, Waning antibody levels and avidity: Implications for MMR vaccine-induced protection. *J. Infect. Dis.* **206**, 1542–1548 (2012).
51. A. P. Fiebelkorn *et al*., "Mumps antibody response in young adults after a third dose of measles-mumps-rubella vaccine" in *Open Forum Infectious Diseases* (Oxford University Press, 2014), vol. 1.
52. C. V. Cardemil *et al*., Effectiveness of a third dose of MMR vaccine for mumps outbreak control. *N. Engl. J. Med.* **377**, 947–956 (2017).
53. F. M. G. Magpantay, M. Domenech De Cellés, P. Rohani, A. A. King, Pertussis immunity and epidemiology: Mode and duration of vaccine-induced immunity. *Parasitology* **143**, 835–849 (2016).
54. A. A. King, M. Domenech, F. M. de Cellès, P Rohani Magpantay, Avoidable errors in the modelling of outbreaks of emerging pathogens, with special reference to ebola. *Proc. R. Soc. B: Biol. Sci.* **282**, 20150347 (2015).
55. M. van Boven, W. L. Ruijs, J. Wallinga, P. D. O'Neill, S. Hahne, Estimation of vaccine efficacy and critical vaccination coverage in partially observed outbreaks. *PLoS Comput. Biol.* **9**, e1003061 (2013).
56. B. D. Elderd, V. M. Dukic, G. Dwyer, Uncertainty in predictions of disease spread and public health responses to bioterrorism and emerging diseases. *Proc. Natl. Acad. Sci. U.S.A.* **103**, 15693–15697 (2006).
57. Census (2019). https://www.census.gov/data/data-tools.html.
58. J. Mossong *et al*., Social contacts and mixing patterns relevant to the spread of infectious diseases. *PLOS Med.* **5**, e74 (2008).
59. Immunization and vaccine-preventable communicable diseases (2019). https://www.who.int/data/gho/data/themes/immunization.
60. D. Anderson, R. Watson, On the spread of a disease with gamma distributed latent and infectious periods. *Biometrika* **67**, 191 (1980).
61. H. J. Wearing, P. Rohani, M. J. Keeling, Appropriate models for the management of infectious diseases. *PLoS Med.* **2**, e174 (2005).
62. A. A. King, D. Nguyen, E. L. Ionides, Statistical inference for partially observed Markov processes via the R package pomp. *J. Stat. Softw.* **69**, 1–43 (2016).
63. O. Diekmann, J. Heesterbeek, M. G. Roberts, The construction of next-generation matrices for compartmental epidemic models. *J. R. Soc. Interface* **7**, 873–885 (2010).
64. D. He, E. L. Ionides, A. A. King, Plug-and-play inference for disease dynamics: Measles in large and small populations as a case study. *J. R. Soc. Interface* **7**, 271–283 (2010).
65. K. Mullen, D. Ardia, D. L. Gil, D. Windover, J. Cline, Deoptim: An R package for global optimization by differential evolution. *J. Stat. Softw.* **40**, 1–26 (2011).
66. J. A. Nelder, R. Mead, A simplex method for function minimization. *Comput. J.* **7**, 308–313 (1965).
67. J. L. Devore, *Probability and Statistics for Engineering and the Sciences* (Cengage Learning, 2011).
68. S. Kullback, R. A. Leibler, On information and sufficiency. *Ann. Math. Stat.* **22**, 79–86 (1951).